138-Tb/s Mode- and Wavelength-Multiplexed Transmission Over Six-Mode Graded-Index Fiber

John van Weerdenburg, *Student Member, IEEE*, Roland Ryf, *Senior Member, IEEE*, Juan Carlos Alvarado-Zacarias, *Student Member, IEEE*, Roberto Alejandro Alvarez-Aguirre, *Student Member, IEEE*, Nicolas Keith Fontaine, *Senior Member, IEEE*, Haoshuo Chen, Rodrigo Amezcua-Correa, *Member, IEEE*, Yi Sun, *Senior Member, IEEE*, Lars Grüner-Nielsen, *Member, IEEE*, Rasmus V. Jensen, Robert Lingle Jr., *Member, IEEE*, Ton Koonen, *Fellow, IEEE*, and Chigo Okonkwo, *Member, IEEE*

(Post-Deadline Paper)

***Abstract*—We report on the multiplexing of 12 spatial and polarization channels and 120 wavelength channels in the *C*-band, each carrying 16 quadratic-amplitude modulation symbols at 30 GBd over graded-index few-mode fiber. A combination of multiple fiber spools with positive and negative modal dispersion values is exploited to form a 59-km link with 0.35-ns differential mode group delay. The link is placed inside a sixfold synchronized recirculating loop transmission setup. Photonic lanterns with low insertion and mode-dependent loss are employed to excite the six spatial modes in the few-mode fiber. A net transmission rate of 138 Tb/s at a spectral efficiency of 34.91 b/s/Hz over 590 km is demonstrated.**

***Index Terms*—Optical fiber communication, space division multiplexing, wavelength division multiplexing.**

I. Introduction

TRAFFIC in optical communication systems has been growing exponentially in recent years, and current forecasts are corroborating this trend for the near future. Technological advances such as transmitting higher order modulated symbols at higher baud rates, constellation shaping (e.g. probabilistic and geometric) and more efficient use of the available optical spectrum has been able to support this increase in capacity demand. However, these techniques are not able to facilitate the traffic growth required as the non-linear Shannon capacity limit of single-mode fiber (SMF) technology is approached [1], [2].

To facilitate this capacity growth, the use of spatially separated channels is proposed. Increasing the spatial multiplicity in a single fiber is favorable as it has the potential to save energy, space, and costs [1], [3]. One approach of space division multiplexing (SDM) in a single fiber is transmitting over multiple modes within a single fiber core [4]–[13], or over multiple cores [14]–[16]. Transmitting over multiple modes in a single fiber has several advantages but is susceptible to transmission effects and impairments, such as differential mode group delay (DMGD) and mode dependent loss (MDL), that do not exist in SMF. As the spatial channels co-exist in the same core, mixing between modes occurs during propagation, which can be resolved by multiple-input multiple-output (MIMO) digital signal processing (DSP). However, different propagation constants for the spatial channels introduce DMGD and results in impulse response broadening, which in turn requires more memory at the receiver in order to successfully unravel the modes. Additionally, MDL can lead to outage, thus limiting capacity of SDM transmission systems [17]. As compensation in DSP is challenging, mitigation of MDL has to be mainly addressed in component design and fabrication.

As the complexity of mode-multiplexed transmission systems scales with the number of modes, fibers supporting a limited number of modes have received lots of interest [4]–[13]. With these few-mode fibers, spectral efficiency as high as 58 bit/s/Hz over single span distances has been demonstrated for 10 modes [11]. Experiments with 3-mode fibers report transmission reach up to 3500 km at lower spectral efficiency of 9 bit/s/Hz [12]. With 6-mode fibers, a higher spectral efficiency over 15 bit/s/Hz was reported at transmission over hundreds of kilometers [8]. Combined with multi-core technology 10 Pb/s transmission over a short length of 11.3 km using both the C and L bands has been recently demonstrated [14]. Although, high throughput

Manuscript received November 6, 2017; revised December 18, 2017; accepted December 22, 2017. Date of publication January 8, 2018; date of current version March 1, 2018. This work was supported in part by the ICT R&D Program of MSIP/IITP, South Korea (R0101-17-0071, Research of MDM optical transmission technology over 10-km multimode fiber) and in part by the Dutch NWO Graduate Photonics Program. *(Corresponding author: John van Weerdenburg.)*

J. J. A. van Weerdenburg, A. M. J. Koonen, and C. M. Okonkwo are with the Institute for Photonic Integration, Eindhoven University of Technology, Eindhoven 5600 MB, The Netherlands (e-mail: j.j.a.v.weerdenburg@tue.nl; a.m.j.koonen@tue.nl; c.m.okonkwo@tue.nl).

R. Ryf, N. K. Fontaine, and H. Chen are with the Nokia Bell Laboratories, Holmdel, NJ 07733 USA (e-mail: roland.ryf@nokia.com; nicolas.fontaine@nokia-bell-labs.com; haoshuo.chen@nokia-bell-labs.com).

J. C. Alvarado-Zacarias, R. A Alvarez-Aguirre, and R. Amezcua-Correa are with the CREOL, The College of Optics and Photonics, University of Central Florida, Orlando, FL 32816 USA (e-mail: jcalvarazac@knights.ucf.edu; roberto.alvarez@knights.ucf.edu; r.amezcua@creol.ucf.edu).

Y. Sun and R. Lingle Jr., are with the OFS, Norcross, GA 30071 USA (e-mail: ysun@ofsoptics.com; rlingle@ofsoptics.com).

L. Grüner-Nielsen is with the Danish Optical Fiber Innovation, Brønshøj 2700, Denmark (e-mail: lgruner@ofsoptics.com).

R. V. Jensen is with the OFS Fitel Denmark, Brøndby 2605, Denmark (e-mail: rjensen@ofsoptics.com).

Color versions of one or more of the figures in this paper are available online at http://ieeexplore.ieee.org.

Digital Object Identifier 10.1109/JLT.2018.2791100

has been demonstrated with few-mode multi-core fiber (FM-MCF), achieving such high throughput over longer FM-MCF transmission distance comparable to single-mode and few-mode fiber (FMF) transmission systems has been elusive. In addition, fabrication of FMF is much simpler than their multi-core counterparts. Hence, key design parameters of mode-multiplexed transmission systems are the fiber design, the spectral efficiency and the maximum transmission reach to optimally exploit all available dimensions.

In this work, we report transmission over graded-index 6-mode FMF at a spectral efficiency of 34.9 bit/s/Hz up to 1475 km [13]. Furthermore, a maximum net transmission rate of 138 Tbit/s over 590 km was demonstrated by means of synchronized recirculating loop setups with 59 km FMF link. To the best of our knowledge, this is the highest throughput-distance product for C-band transmission in a single core few-mode fiber reported to date. These results are obtained by loading 120 wavelength channels multiplexed in 2 polarizations and 6 spatial modes with 120 Gbit/s mapped to 16-QAM symbols. Long distance results are enabled by combining positive and negative dispersion fibers to reduce the total DMGD of the link to approximately 6 ps/km, and by using photonic lantern mode multiplexers with low mode dependent and insertion losses.

This paper is organized as follows: In the next section the design of the fiber and the characterization of the transmission link are described. Section III covers the design, manufacturing process and characterization of the photonic lantern mode multiplexers. In Section IV, we describe the 6-mode transmission experimental setup. Section V covers the experimental results, where the performance is assessed in terms of Q-factor and in terms of maximum transmission reach given the wavelength dependent mode-dependent losses of the system. We discuss in particular the Q-factor for specific transmission distances given the specific recirculating loop round-trips.

II. 6-Mode Graded-Index Fiber

The FMF supports exactly 4 linear polarized (LP) modes [8], namely LP_{01}, LP_{11}, LP_{21}, and LP_{02}. Because both LP_{11} and LP_{21} each have 2 degenerate modes, labeled with 'a' and 'b', 6 spatial modes each with 2 polarizations are available for SDM transmission. All supported modes have an attenuation of 0.2 dB/km, while the chosen normalized frequency (or V-parameter) ensures cut-off of higher order modes. The refractive-index profile is of the graded-index type and is optimized to minimize DMGD between the 4 mode-groups. Effective areas of 90 μm^2 for the LP_{01}, 120 μm^2 for the LP_{11} modes, 165 μm^2 for LP_{21} and 180 μm^2 for the LP_{02} mode, respectively, increases its tolerance towards non-linear transmission effects, thus allowing higher transmission powers with respect to standard single-mode fiber (SSMF). The chromatic dispersion (CD) is close to conventional SSMF with approximately 18 ps/(nm km) averaged over all the modes.

Although the fiber is designed to have low DMGD, the total mode dispersion in a link can be further reduced by combining multiple fiber spools with positive and negative dispersion values [5]. This technique is similar to chromatic dispersion compensation with dispersion compensated fiber (DCF), however for mode division multiplexing (MDM) transmission dispersion between all modes has to be minimized. For this setup, the 4 reels described in Table I are fusion spliced to form a 59 km link with a final mode-group dispersion of 0.35 ns. The dispersion map in Fig. 1 shows the evolution of the mode dispersion in the link. For simplification, a linear dispersion growth is assumed, which is true for weakly-coupled multi-mode transmission systems. From the figure, it can be seen that the maximum DMGD at any point in the fiber link is below the largest value of the individual fiber spools as specified in Table I. The effect of DMGD compensation is also visible in the impulse response of the system, obtained by averaging over all elements of the 12×12 MIMO channel estimation [6]. Fig. 2 shows the impulse response after 1, 3, and 10 circulations. After transmission over one span, most energy is concentrated in a window of approximately 1 ns. The side peaks, correspond to the modal dispersions at the splice points within the fiber link and are at least 20 dB suppressed. As the full impulse response can still

TABLE I
Lengths and DMGDs of the Spools in the Few-Mode Link

Spool	L [km]	DMGD [ns]		
		LP_{01}-LP_{11}	LP_{01}-LP_{21}	LP_{01}-LP_{02}
1	3.0	-1.60	-3.19	-3.26
2	30.0	3.17	8.56	8.56
3	19.3	-0.70	-3.14	-3.31
4	6.5	-0.67	-1.88	-1.82
Total	58.8	0.20	0.35	0.16

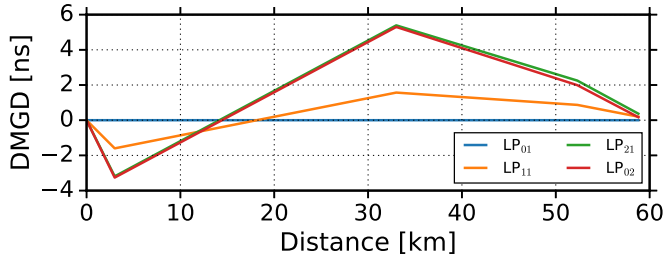

Fig. 1. Dispersion map of DMGD managed 59 km fiber link showing the build up and compensation of mode-group delay to 0.35 ns.

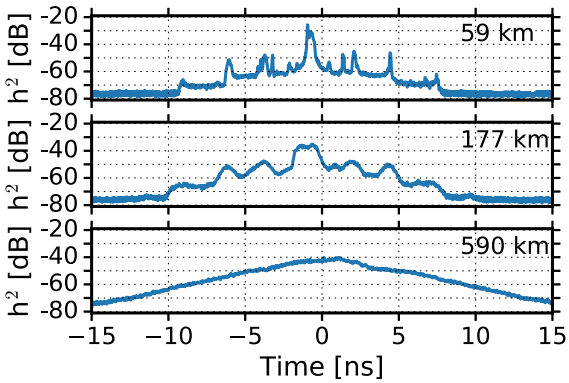

Fig. 2. Intensity averaged impulse responses after 59, 177, and 590 km transmission obtained by channel estimation.

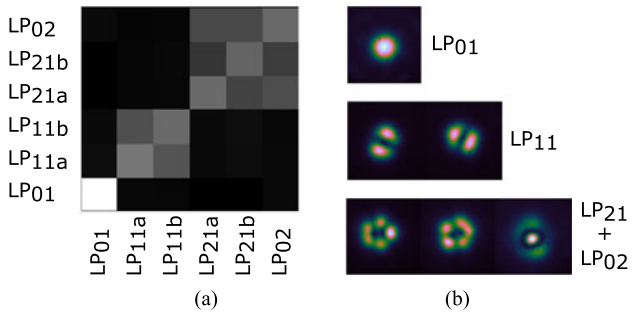

Fig. 3. (a) Transfer matrix of the photonic lantern mode multiplexer indicating high intensity within the three mode-groups and limited crosstalk between the groups. (b) Mode profiles captured with an NIR camera.

be captured within the 30 ns wide equalizer window it is not expected that transmission performance is limited by dispersion at a range of 590 km.

III. Mode-Selective Photonic Lanterns

To excite the modes in the transmission fiber, photonic lantern (PL) are employed. These fiber based mode multiplexers can be fabricated with low mode dependent and insertion losses, and can be fusion spliced to the transmission fiber to minimize coupling losses [18]. 6 SMF are positioned within a low refractive capillary, which is heated and pulled to adiabatically taper the structure down to match the dimensions of the FMF. In the tapered section, the light escapes from the SMF cores and it will form a super-mode. Note that the first photonic lanterns did not have a strong relation between input fibers and excited modes, which made launch power control challenging. To introduce mode selectivity, the mode degeneracy can be broken by using distinct propagation constants for each input [19]. In our design, dissimilar SMF with core radii of 23 μm, 18 μm, 15 μm, and 11 μm were selected for LP_{01}, LP_{11}, LP_{21}, and LP_{02} respectively [20].

Both multiplexers are characterized after manufacturing with an optical vector network analyzer (OVNA) [21]. From the measured transfer functions, MDL and mode selectivity are obtained. We found an MDL of 1.3 and 2.0 dB for our devices. The transfer matrix depicted in Fig. 3(a) shows coupling between the spatial channels as intensity. In this matrix, mixing within the degenerate modes of LP_{11} and LP_{21} can be seen. As well as a coupling between the LP_{21} and LP_{02} modes due to similar propagation constants, which is also visible from the overlapping curves in Fig 1. Limited crosstalk between the three mode-groups was observed. Another indication of mode selectivity comes from observing the few-mode output with a near infrared (NIR) camera. In the profiles in Fig. 3(b) the LP mode profiles are clearly recognizable.

Next, a short length of 6-mode fiber is fusion spliced to the multiplexers and the performance is once again evaluated. For this test amplified spontaneous emission (ASE) is injected in one of the SMF inputs of the PL while observing the power at the FMF facet. The received optical power measured at the end of each multiplexer, and after splicing one multiplexer to the transmission fiber are given in Table II. The average loss of the fiber is estimated to be 0.22 dB/km and less than 2 dB variation in insertion loss (IL) for the full link was observed. This offset can be easily compensated during transmission by controlling the individual launch powers.

TABLE II
Insertion Losses of the Mode Multiplexers and the 59 km FMF Span

Mode	Insertion loss [dB]			
	MUX	DEMUX	59km FMF	Total
LP_{01}	0.59	1.93	12.99	15.51
LP_{11a}	0.76	0.80	12.84	14.40
LP_{11b}	0.38	3.20	13.17	17.34
LP_{21a}	2.30	0.87	13.30	17.06
LP_{21b}	0.79	0.91	13.54	15.83
LP_{02}	1.57	1.56	13.43	17.15

IV. Few-Mode Transmission Setup

In the transmission setup illustrated in Fig. 4 a 33 GHz spaced grid of 120 wavelength channels is generated by modulating the output of 40 distributed feedback (DFB) lasers with a 33.3 GHz tone. The odd and even channels of the grid are separated and independently modulated by nested Mach-Zehnder modulator (MZM). The modulators are driven by two digital to analog converter (DAC) running at 60 GS/s, which produce a sequence of 2^{16} 16-QAM De Bruijn symbols. Polarization multiplexing is simulated by adding fiber delay to one input of a polarization beam splitter (PBS). Throughout this transmitter sub-system erbium doped fiber amplifier (EDFA) compensate for any losses, while a gain flattening filter (GFF) enforces a flat spectrum, minimizing performance differences between wavelength channels. In a wavelength selective switch (WSS) one of the channels is replaced with the channel under test (ChUT), which is modulated with independent data by a similar transmitter setup.

For long distance transmission experiments the signals are transmitted trough a loop setup. This setup combines multiple conventional SMF recirculating loops with a shared multi-mode link. On each path in the loop there is a 1×2 solid state switch to switch between loading and looping states, a splitter to redirect 10% of the signal to the receiver, 2 stage EDFA, and GFF. In between the 2 stages of the EDFA are the mode multiplexers and DMGD minimized 59 km 6-mode fiber span. The path lengths are matched within centimeters of each other and any variation in losses is compensated for by tuning variable optical attenuator (VOA) of the 2-stage EDFA. Furthermore, all loop switches are synchronized and one extra switch is placed before the mode decorrelation to improve extinction ratio. The 98 ns decorrelation delays are sufficiently long to avoid overlap within the equalizer windows of the spatial tributaries [22].

The outputs of the loop are amplified and passed through WSS where the loading channels are dropped before sending the channels of interest to the receivers. A 10 KHz linewidth external cavity laser (ECL) is tuned to match the wavelength of the ChUT and acts as a local oscillator (LO) signal for the 6 polarization diverse coherent receiver (PD-CRX). The receiver outputs are converted to the digital domain by a 20 GHz

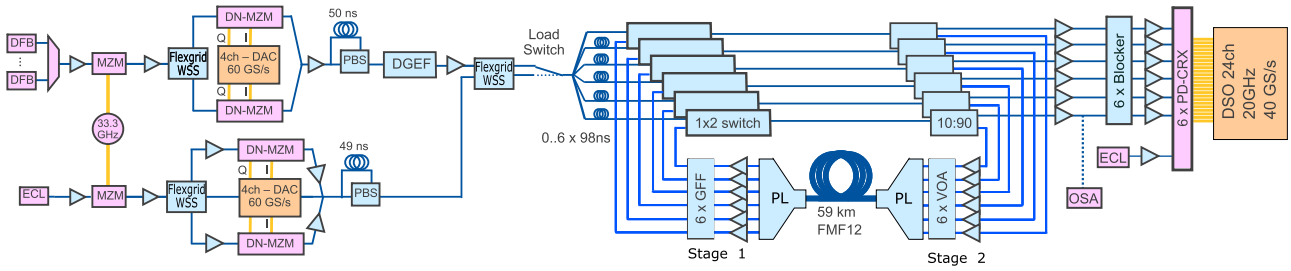

Fig. 4. Few-mode recirculating loop transmission setup. Triangles represent EDFAs.

bandwidth, 24 channel real-time oscilloscope operating at 40 GS/s. Alternatively, the outputs of the loop can be redirected to an optical spectrum analyzer (OSA) for analyzing the spectrum.

All signal processing is performed offline [23]. First, all signals are aligned in time and resampled to 2-fold oversampling. Next, IQ-imbalance, CD, and frequency offset between signal and LO are compensated. Subsequently, a 12 × 12 MIMO frequency domain equalizer (FDE) is applied to undo the mode mixing. This equalizer combines the least means square (LMS) algorithm for convergence with a multi-modulus algorithm (MMA) during transmission. The last block in the DSP chain recovers the carrier phase before performance is evaluated over 8 million bits per spatial channel.

V. Transmission Results

This result section is split into two subsections. In the first we describe the optimization of the transmission setup using only 15 of the 120 wavelength channels centered around 1550 nm, reducing both measurement and processing time significantly. In the second section, all 120 wavelength channels are enabled to achieve 138 Tbit/s.

A. System Optimization and 15 WDM Channel Transmission

At first, any performance variation amongst the spatial channels is investigated by varying the launch power in one of the PL inputs. A 2 dB offset for one of the LP_{21} modes was observed, which matches with earlier IL measurements described in Table II. This offset can be easily compensated by tuning the VOA inside the loop. With this optimization applied, all spatial channels perform similarly over the measured range of powers and all have their optimum around −1 dBm, as can be seen in Fig. 5.

Next, we investigate the performance of the system for various transmission distances while sweeping the launch power. The Q-factors after 118, 295, 590, 885, 1180, and 1475 km are depicted in Fig. 6. Any difference in Q-factor between the spatial channels is represented by the shaded area, while the solid line indicates the system average. Note that after 1475 km transmission the averaged Q-factor is approximately 6 dB at the optimum, enabling transmission when 20% overhead soft decision forward error correction (SD-FEC) is assumed, resulting in a record spectral-efficiency-distance product of 51,400 bit/s/Hz × km. Although the worst performing spatial channels are on the edge of the assumed forward error correction (FEC) threshold, a simple space-time coding scheme such as round-robin coding [10] can be applied to equalize performance to the system average.

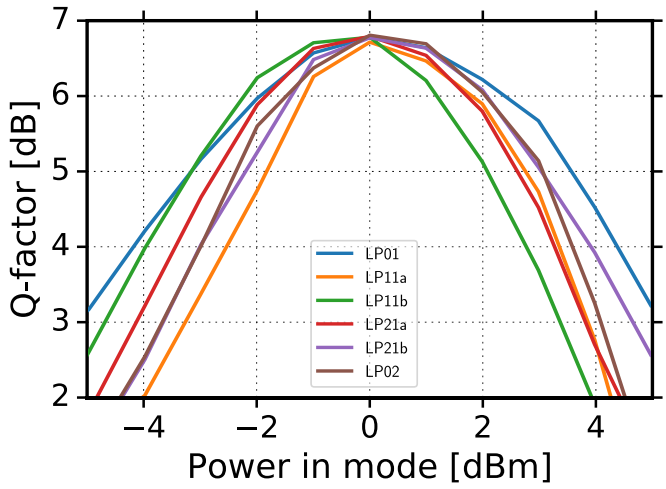

Fig. 5. Q-factors of the spatial modes versus launch power after 590 km transmission.

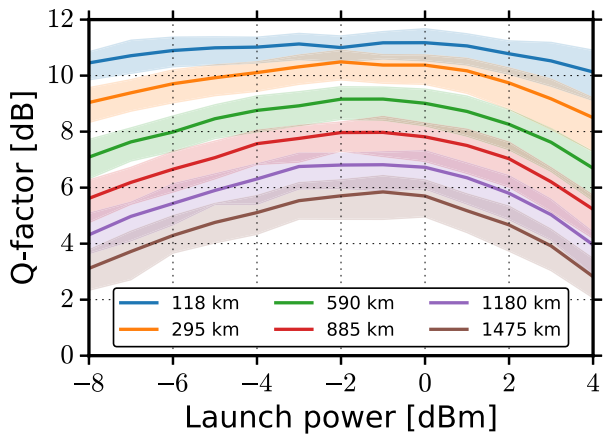

Fig. 6. Q-factors versus launch power for various transmission distances. Solid line represents the system average, while the shaded areas indicate the performance difference of the spatial channels.

For each wavelength channel, the 12 × 12 transfer matrix is estimated by the MIMO equalizer. A singular value decomposition (SVD) performed on this matrix returns the strengths of the 12 transmission channels in the form of singular values. Typically the MDL is represented as the ratio between the strongest and weakest singular value. These values are calculated for each distance captured, also points after the maximum transmission

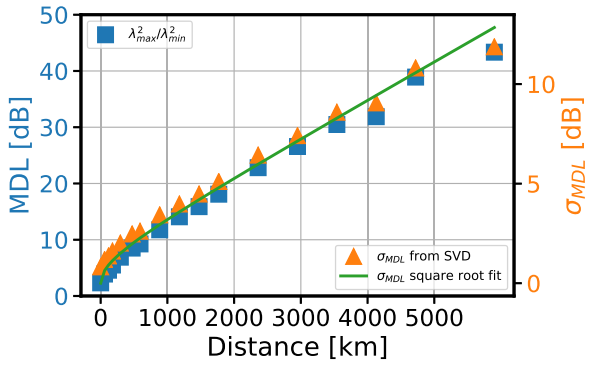

Fig. 7. Mode dependent loss calculated as ratio between strongest and weakest singular value as well as the standard deviation of the MDL and its square root fit function.

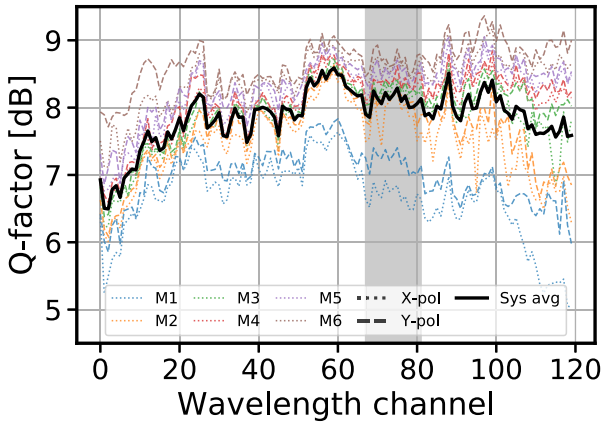

Fig. 8. Q-factors of the wavelength channels. Solid black line represents the system average, while dotted and dashed lines show the performance difference of the spatial channels for the two polarizations. The 15 wavelength channels in the gray shaded area corresponds to channels used in the experiments of Section V-A.

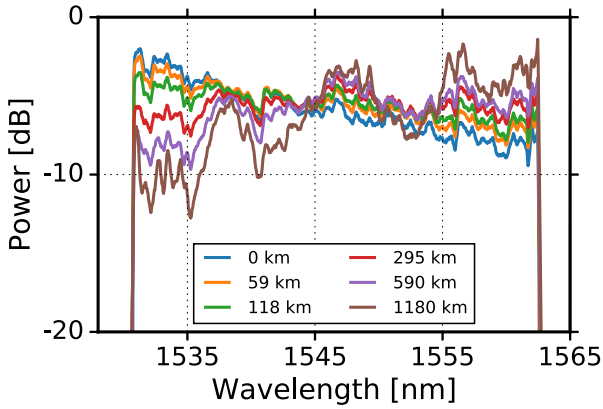

Fig. 9. Optical spectrum shows a tilting effect increasing with transmission distances.

reach are included, as can be seen in Fig. 7. We observe a MDL of 3.9 dB after the first circulation, which corresponds closely to the measured 1.3 and 2.0 dB MDL of the mode multiplexers, leaving a residual MDL of approximately 0.01 dB/km for the fiber. Another interesting parameter can be calculated from the SVD, namely the standard deviation of the MDL. This parameter grows according to

$$\sigma_{MDL} = \xi\sqrt{1+\frac{1}{12}\xi^2} \tag{1}$$

with $\xi = \sqrt{K}\sigma_g$, where K is the number of identical fiber sections, and σ_g is the MDL standard deviation of a single section [17]. As we transmit multiple times over the same span in the recirculating loop setup, the standard deviation of the MDL of the 59 km fiber link can be estimated by fitting the measured standard deviations to (1). As can be seen in Fig. 7, the fitted curve matches closely to the calculated values for $\sigma_g =$ is 0.62 dB.

B. 138 Tbit/s Transmission

For the next experiment, we maximize throughput of the system by modulating 120 wavelength channels at a spacing of 33 GHz, thereby occupying up to 4 THz of bandwidth in the C-band. From the power sweep, we observe no significant changes of optimum launching conditions with respect to earlier experiments. However, a penalty of approximately 1 dB in Q-factor is observed for same 15 wavelength channels previously evaluated. These wavelength channels are highlighted with the gray area in Fig. 8. Moreover, from Fig. 8 lower performance for the shorter wavelengths can be observed, which limits the transmission reach of our system to 590 km. At this distance Q $>$ 6.3 dB still allows for successful signal demodulation when a 20% overhead FEC is applied. The lower performance for the shorter wavelength channels can be attributed to the limited gain for this wavelength regime of the EDFA used to amplify the LO and the non-flat spectrum. A tilting effect of the spectrum increasing with distance was observed from OSA captures, as can be seen in Fig. 9. Note that the OSA has to be synchronized with the recirculating loop, significantly reducing the length of the acquisition windows. The OSA observes only one of the outputs of the recirculating loop, which will contain a combination of the 12 transmitted spatial and polarization channels. This combination might vary with wavelength or over time due to changes in mode mixing. As a result, the spectrum depicted in Fig. 9 does not represent the full multi-mode spectrum at a single moment in time.

In Fig. 8 it can be seen that the spread in performance expressed in Q-factors, of the spatial channels is larger at both ends of the spectrum. This effect is also visible in the calculated MDL in Fig. 10(b). All singular values of the SVD on the estimated transfer matrix of each received wavelength channel are concatenated to form the graph in Fig. 10(a). As there is no data in the guard bands, we do not have information on the MDL at this part of the spectrum. This can be seen in more detail in the close up around 194.0 Thz in Fig. 10(c). Note that, the SVD returns the singular values ordered from strongest to weakest, but do not necessarily represent the same spatial channel for each individual point in the spectrum. Within each wavelength channel the ratio between the strongest and weakest singular value as well as the standard deviation are plotted as the MDL in Fig. 10(b). Plugging in our previously found σ_g 0.62 dB,

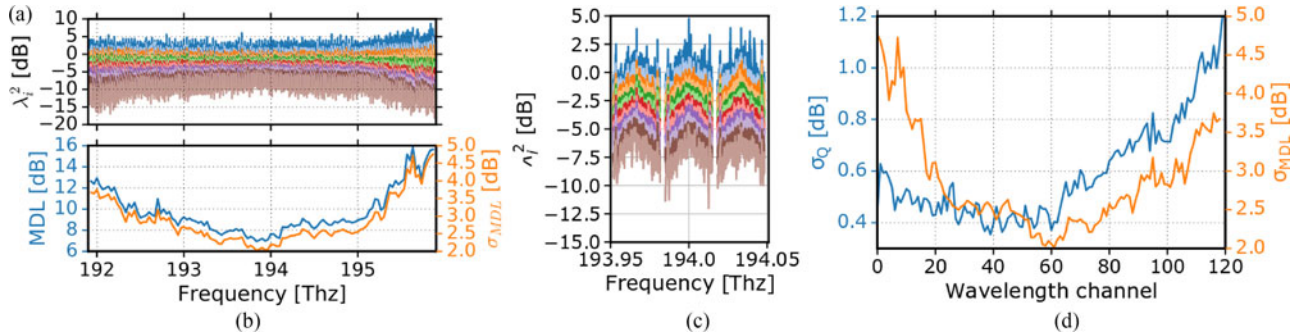

Fig. 10. (a) Singular values obtained by SVD of the transfer matrix of each wavelength channel. Each color represents a single λ_i^2. (b) Mode dependent loss calculated as ratio between strongest and weakest singular value as well as the standard deviation of the MDL. (c) close-up if figure a, centered around 194 THz. (d) Standard deviation of spatial channel Q-factors and mode dependent loss.

a standard deviation of 2.9 dB in MDL is expected. As can be seen in Fig. 10(b) this is true for center wavelengths that were investigated earlier, but does not hold for the ends of the spectrum.

Fig. 10(d) shows both the standard deviation in Q-factor and MDL. Please be aware that the x-axis represents wavelength and not frequency as in Fig. 10(b). It can be seen that for the channels in the longer wavelengths these curves show similar trends, and it can be assumed that the transmission performance for those wavelength channels are mainly limited by the mode dependent loss of the system.

VI. Conclusion

We have reported a spectral-efficiency distance product over 50,000 bits/s/Hz × km by transmitting 15 wavelength, and 12 spatial and polarization channels modulated with 120 Gbit/s 16-QAM in 500 GHz of bandwidth over 1475 km. By increasing the number of wavelength channels to 120, a net transmission throughput of 138 Tbit/s over 590 km was achieved in a single core. These results demonstrate the potential of MDM to overcome the capacity crunch for long-haul transmission systems.

References

[1] P. J. Winzer and D. T. Neilson, "From scaling disparities to integrated parallelism: A decathlon for a decade," *J. Lightw. Technol.*, vol. 35, no. 5, pp. 1099–1115, Mar. 2017.

[2] R.-J. Essiambre, G. Kramer, P. J. Winzer, G. J. Foschini, and B. Goebel, "Capacity limits of optical fiber networks," *J. Lightw. Technol.*, vol. 28, no. 4, pp. 662–701, Feb. 2010.

[3] D. J. Richardson, J. M. Fini, and L. E. Nelson, "Space-division multiplexing in optical fibres," *Nature Photon.*, vol. 7, pp. 354–362, Apr. 2013.

[4] C. Koebele *et al.*, "40 km transmission of five mode division multiplexed data streams at 100 Gb/s with low MIMO-DSP complexity," in *Proc. 37th Eur. Conf. Expo. Opt. Commun.*, Washington, DC, USA: Opt. Soc. Amer., 2011, Paper Th.13.C.3. [Online]. Available: http://www.osapublishing.org/abstract.cfm?URI=ECOC-2011-Th.13.C.3

[5] S. Randel *et al.*, "Mode-multiplexed 6x20-GBd QPSK transmission over 1200-km DGD-compensated few-mode fiber," in *Proc. Opt. Fiber Commun. Conf./Nat. Fiber Opt. Eng. Conf.*, Mar. 2012, pp. 1–3.

[6] R. Ryf *et al.*, "Mode-multiplexed transmission over a 209-km DGD-compensated hybrid few-mode fiber span," *IEEE Photon. Technol. Lett.*, vol. 24, no. 21, pp. 1965–1968, Nov. 2012.

[7] V. Sleiffer *et al.*, "73.7 Tb/s (96 × 3 × 256-Gb/s) mode-division-multiplexed DP-16QAM transmission with inline MM-EDFA," *Opt. Express*, vol. 20, no. 26, pp. B428–B438, Dec. 2012. [Online]. Available: http://www.opticsexpress.org/abstract.cfm?URI=oe-20-26-B428

[8] R. Ryf *et al.*, "708-km combined WDM/SDM transmission over few-mode fiber supporting 12 spatial and polarization modes," in *Proc. 39th Eur. Conf. Exhib. Opt. Commun.*, Sep. 2013, pp. 1–3.

[9] E. Ip *et al.*, "146λ × 6 × 19-Gbaud wavelength-and mode-division multiplexed transmission over 10 × 50-km spans of few-mode fiber with a gain-equalized few-mode EDFA," *J. Lightw. Technol.*, vol. 32, no. 4, pp. 790–797, Feb. 2014. [Online]. Available: http://jlt.osa.org/abstract.cfm?URI=jlt-32-4-790

[10] J. van Weerdenburg *et al.*, "10 Spatial mode transmission using low differential mode delay 6-LP fiber using all-fiber photonic lanterns," *Opt. Express*, vol. 23, no. 19, Sep. 2015, Art. no. 24759.

[11] H. Chen *et al.*, "High spectral efficiency mode-multiplexed transmission over 87-km 10-mode fiber," *Opt. Fiber Commun. Conf.*, 2016, Paper Th4C.2.

[12] G. Rademacher *et al.*, "3500-km mode-multiplexed transmission through a three-mode graded-index few-mode fiber link," in *Proc. 43rd Euro. Conf. Opt. Commun.*, Sep. 2017, Paper M.2.E.4.

[13] J. van Weerdenburg *et al.*, "138 Tbit/s transmission over 650 km graded-index 6-mode fiber," in *Proc. 2017 43rd Eur. Conf. Opt. Commun.*, Sep. 2017, Paper Th.PDP.A.4.

[14] D. Soma *et al.*, "10.16 peta-bit/s dense SDM/WDM transmission over low-DMD 6-mode 19-core fibre across C+L band," in *Proc. 2017 43rd Eur. Conf. Opt. Commun.*, Sep. 2017, Paper Th.PDP.A.1.

[15] K. Igarashi *et al.*, "114 space-division-multiplexed transmission over 9.8-km weakly-coupled-6-mode uncoupled-19-core fibers," in *Proc. 2015 Opt. Fiber Commun. Conf. Exhib.*, Mar. 2015, pp. 1–3.

[16] T. Sakamoto *et al.*, "Low-loss and low-DMD few-mode multi-core fiber with highest core multiplicity factor," in *Proc. 2016 Opt. Fiber Commun. Conf. Exhib.*, Mar. 2016, pp. 1–3.

[17] K.-P. Ho and J. M. Kahn, "Mode-dependent loss and gain: Statistics and effect on mode-division multiplexing," *Opt. Express*, vol. 19, no. 17, pp. 16612–16635, Aug. 2011.

[18] T. A. Birks, I. Gris-Sánchez, S. Yerolatsitis, S. G. Leon-Saval, and R. R. Thomson, "The photonic lantern," *Adv. Opt. Photon.*, vol. 7, no. 2, pp. 107–167, Apr. 2015.

[19] S. G. Leon-Saval, N. K. Fontaine, J. R. Salazar-Gil, B. Ercan, R. Ryf, and J. Bland-Hawthorn, "Mode-selective photonic lanterns for space-division multiplexing," *Opt. Express*, vol. 22, no. 1, pp. 1036–1044, Jan. 2014.

[20] A. M. Velazquez-Benitez *et al.*, "Six spatial modes photonic lanterns," in *Proc. Opt. Fiber Commun. Conf.*, 2015, Paper W3B.3.

[21] N. K. Fontaine *et al.*, "Characterization of space-division multiplexing systems using a swept-wavelength interferometer," in *Proc. Opt. Fiber Commun. Conf./Nat. Fiber Opt. Eng. Conf.*, 2013, Paper OW1K.2.

[22] A. Sierra, S. Randel, P. J. Winzer, R. Ryf, A. H. Gnauck, and R. J. Essiambre, "On the use of delay-decorrelated I/Q test sequences for QPSK and QAM signals," *IEEE Photon. Technol. Lett.*, vol. 24, no. 12, pp. 1000–1002, Jun. 2012.

[23] M. S. Faruk and K. Kikuchi, "Adaptive frequency-domain equalization in digital coherent optical receivers," *Opt. Express*, vol. 19, no. 13, pp. 12 789–12 798, Jun. 2011. [Online]. Available: http://www.opticsexpress.org/abstract.cfm?URI=oe-19-13-12789

Authors' biographies not available at the time of publication.